EFFECT OF ION IMPLANTATION ON THERMAL SHOCK RESISTANCE OF MAGNESIA AND GLASS

V. N. Gurarie

School of Physics, University of Melbourne ,

Parkville, VIC, 3052, Australia.

J. S. Williams and A. J. Watt

Department of Electronic Materials Engineering, Research School of Physical Sciences and Engineering, ANU, Canberra 2600, Australia.

Monocrystals of magnesia together with glass samples have been subjected to ion implantation prior to thermal shock testing in an impulse plasma of continuously varied intensity. Measurements of the separation between fragments have been used to estimate the surface temperature. Fracture and deformation characteristics of the surface layer are measured in ion implanted and unimplanted samples using optical and scanning electron microscopy. Implantation-induced near-surface damage is analysed by ion channeling using 2 MeV He^+ ions. Ion implantation is shown to modify the near-surface structure of magnesia samples by introducing damage, which makes crack initiation easier under thermal stresses. The fracture threshold and maximum crack density are shifted towards the lower temperature range. Ion implanted MgO crystals show a ten fold increase in surface crack density. An increased crack density results in a decreased degree of damage characterised by the depth of crack penetration. The thermal stress resistance parameter of glass samples is increased at relatively small doses and decreased at higher doses. The results suggest that crack density and the degree of fracture damage in brittle ceramics operating under thermal shock conditions can be effectively controlled by ion implantation which provides crack initiating defects in the near-surface region.

1. INTRODUCTION

Ceramic materials are widely used in high temperature technology because of their high

melting point and ability to retain strength up to high temperature. However, they are commonly brittle and are easily fractured by dynamic stresses arising under thermal shock loading. This often limits their application and hampers progress in a variety of high temperature technologies. The thermal shock fracture behaviour of materials is a subject of intensive study[1-6]. It is known that thermal shock-induced fracture mainly originates at the surface, where maximum tensile stresses first appear, and then cracks propagate into the sample interior[7,8]. Cracks commonly initiate at surface defects such as cleavage steps, microcracks, scratches, twins, grain boundaries and other surface inhomogeneities[9,10]. Thus, the response to thermal shock essentially depends on the state of the surface and material surface properties. Surface modification by ion implantation has been shown to alter a number of strength and fracture characteristics of lithium fluoride crystals exposed to thermal stress loading[11]. In particular, the fracture threshold is lowered by ion implantation, allowing fracture to be initiated at lower surface temperatures. At the same time, ion implantation produces a higher density of cracks in LiF , but such cracks penetrate smaller distances into the material. This effectively raises the damage resistance parameter[12-14] and therefore should result in higher durability following damage by thermal shock.

The aim of the present paper is to identify and characterise the effect of ion implantation on thermal stress fracture behaviour of glass samples and monocrystals of magnesia. The investigation includes surface characterisation using optical and scanning electron microscopy, which provides qualitative and quantitative information on the surface fracture temperature, fracture threshold, crack pattern morphology, crack density and fragment size. These characteristics are studied as a function of intensity of thermal shock testing at various implantation doses. The degree of ion implantation damage in MgO monocrystals is monitored by ion channeling and the degree of damage correlated with fracture properties. Thus, the effect of ion implantation on thermal stress resistance parameters is discussed in the light of ion-beam damage and its effect on materials characteristics and properties.

2. EXPERIMENTAL METHOD

MgO monocrystals with the (100) face and soda-lime, plate glass samples were implanted

with 70 KeV Si^- ions at room temperature to doses ranging from $5x10^{14}$ cm^{-2} to $5x10^{16}$ cm^{-2}. Only half of the crystal surface was subjected to implantation to compare the response to thermal shock of implanted and unimplanted regions. Following implantation the MgO monocrystals were analysed by ion channeling, using 2 MeV He^+ ions, to measure implantation-induced near-surface damage.

Thermal shock was produced by exposing the sample surface of ~ 1.5 x 3 cm^2 to a plasma jet obtained by an electrical discharge[15]. The discharge was produced using 4 kV, 500 μF capacitor system. Electrical characteristics of the discharge were deduced from the e.m.f. waveform generated in an inductively coupled loop. A heavily damped oscillatory discharge occurred with ~98% of the energy being released during the first 40 μs. The samples were placed at some distance from the plasma gun with the plasma jet propagating perpendicular to the sample surface. The temperature distribution on the sample surface had a radial symmetry with its central hot spot located on the border between implanted and unimplanted regions. Thus, both implanted and unimplanted regions were under similar temperature conditions. The heat flux and temperature at the sample surface were gradually reduced in the radial direction from this central hot spot. Therefore, this method of heat pulsing allows sample testing under a wide and continuous range of heat intensities. Optical photographs of the fracture patterns of MgO crystal and glass, subjected to plasma testing, are shown in Fig. 1. They illustrate a high degree of fragmentation of the surface layer by cracks following thermal shock.

In these experiments the surface temperature was deduced from the measurements of the separation between fragments. These gaps between the fragments are formed as a result of the contraction of each fragment while cooling from the fracture temperature. Thus, by the end of cooling a relative temperature deformation of the fragment is $\Delta a/a$, where Δa is the gap width and a is the fragment size. On the other hand, the relative temperature deformation is known to be equal to $\Delta a/a = \alpha (T_f - T_o)$, where α is the thermal expansion coefficient, T_f is the fracture temperature, at which a crack separating adjacent fragments originates, and T_o is

the initial sample temperature. The fracture temperature is then determined from the expression: $T_f = T_o + \Delta a / a\,\alpha$. This approach is obviously adequate for brittle materials, which do not exhibit plastic deformation on cooling below the fracture temperature. Experimentally Δa and a were measured as a sum, $\Delta a = \Sigma \Delta a_i$ and $a = \Sigma a_i$, over several fragments, since cracks do not originate simultaneously. The gaps between fragments are often very small, particularly between small fragments and at low peak temperatures. Fig. 2 shows SEM micrographs of MgO and glass samples where the gaps between adjacent fragments are clearly resolved.

The dependence of the fracture temperature, determined by the above method for MgO crystals, on the distance x from the central hot spot of the plasma affected area is shown in Fig. 3. The temperature dependence of α for MgO is also taken into account[16]. One can see from the graph that the fracture temperature is not changed appreciably within a radius of $r \approx 5$ mm of the central hot spot, but is continuously reduced for $r > 5$ mm. The fracture temperature T_f can be shown to be related to the peak temperature T according to the expression[11]: $T_f = T - [(1-\mu)\,\sigma_y + \varepsilon_p E] / \alpha E$, where μ is Poisson's coefficient, σ_y is compressive yield stress, ε_p is the plastic strain prior to fracture and E is Young's modulus. For brittle solids at thermal shock peak temperatures below the brittle-ductile transition, the plastic strain ε_p prior to fracture is small. In this case, ignoring ε_p, we have $T_f = T - (1-\mu)\,\sigma_y / \alpha E$. It is worth noting that the term $(1-\mu)\,\sigma_y / \alpha E$ is of the order of 10^0 - $20\,^0$C for many ceramic materials, which is within the error of these measurements. However, at temperatures above the brittle-plastic transition there is a plastic deformation prior to fracture: $\varepsilon_p = \alpha (T - T_b)$, where T_b is the brittle-ductile transition temperature. This yields the fracture temperature $T_f = T_b - (1-\mu)\,\sigma_y / \alpha E$, which is independent of the peak surface temperature T. This effect is seen in the graph in Fig. 3, where the fracture temperature remains almost

constant in the range between 1700 ^{0}C - 1900 ^{0}C, and obviously corresponds to the brittle-ductile transition for MgO crystals. At r > 5 mm the curve is approximated by a linear dependence, shown in the graph. In the central hot part of the plasma affected area, r < 5 mm, the peak surface temperature was evaluated by means of an extrapolation of the linear dependence into the region r < 5 mm.

3. RESULTS AND DISCUSSION

The experimental results demonstrate that ion implantation affects a number of strength and fracture characteristics of brittle solids: crack density, minimum fragment size, the temperature threshold of cracking and the temperature corresponding to maximum crack density. However, the extent and the direction in which these characteristics change depend on material properties and the implantation dose.

The dependence of crack density on the peak surface temperature for MgO crystals is shown in Fig. 4. Crack density is measured as the number of fragments, separated by cracks, per unit surface area. Both curves, related to ion implanted and unimplanted samples, demonstrate the occurrence of a maximum crack density, observed at some temperature. Similar behaviour was earlier reported for LiF crystals[11]. These maxima are obviously related to the brittle-ductile transition. At temperatures below the brittle-plastic transition an increasing peak temperature increases the fracture temperature and hence the temperature interval available for fragmentation. This should enhance fragmentation. However, the increasing peak temperature above the brittle-ductile transition increases plastic deformation prior to fracture on cooling. As a consequence, the fracture temperature remains practically constant in this temperature range as illustrated by the graph in Fig. 3. In this case fracture starts when a heating/cooling wave penetrates deeper into a sample. This reduces the temperature gradient and thermal stresses during the fragmentation process. Therefore, when the peak temperature exceeds the brittle-ductile transition temperature the final crack density should decrease, which corresponds to the descending right hand branch of the fragmentation curve in Fig. 4. The graph in Fig. 4 also indicates that the maximum of the crack density curve for the implanted crystal is shifted towards lower temperatures.

Ion implanted samples show a much higher degree of fragmentation than the unimplanted ones, particularly at high doses. This effect is illustrated by the photographs in Fig.1 for MgO and glass samples, where ion-implanted and unimplanted regions were exposed to identical thermal shock conditions. The effect of the implantation dose on the maximum crack density for MgO is given in Fig. 5. The graph demonstrates that the difference in crack density between ion implanted and unimplanted zones is still significant at a relatively small dose of $5x10^{14}$ cm^{-2}. High implantation doses result in an almost ten fold increase in the fragment density. At doses of $3x10^{16}$ cm^{-2} and higher the crack density increases more slowly.

Ion implantation is observed to lower the temperature at which fracture starts. Thus, the thermal shock resistance parameter, which represents the minimum temperature variation required to initiate fracture, is decreased following ion implantation of MgO crystals. The difference in the temperature threshold of cracking for unimplanted and implanted regions was measured to vary by up to 600 ^0C for different samples and doses. However, all samples, implanted within the range from $5x10^{14}$ cm^{-2} to $5x10^{16}$ cm^{-2} , display lower temperature thresholds of cracking than those for unimplanted ones. At the smallest dose used, $5x10^{14}$ cm^{-2}, the effect of ion implantation on the threshold of cracking is still very pronounced.

Ion implantation causes measurable lattice disorder in crystalline materials, even at extremely low doses (~ 10^{14} cm^{-2}) where the concentration of implanted species is considerably less than 1 atomic percent[17]. In the case of MgO monocrystals, the clearly observable effect of low dose Si implantation on thermal stress-induced crack propagation suggests that it is lattice damage and not the presence of the Si implanted species which is giving rise to the observed effect. Ion channeling is an ideal technique for measuring lattice disorder produced by ion implantation in monocrystals. In Fig. 6 we show ion channeling spectra illustrating the build up of lattice disorder in MgO with increasing ion dose. The dashed spectrum indicates unimplanted MgO taken with the incident He+ analysis beam aligned with the <100> axial channel normal to the surface. Under such conditions the backscattered yield is low and shows peaks at about channels 175 and 262 which represent O and Mg at the surface, respectively. Also shown is the random spectrum (where the incident beam was intentionally misaligned away from any major crystal direction). In this case the yield is high (showing no

influence of crystal structure) and indicates Mg and O plateaux. Channeling spectra from Si implanted MgO fall between the random and (unimplanted) channeled spectra. This indicates that Si implantation has given rise to lattice displacements and disorder in MgO which tend to randomise the lattice. As shown, damage increases with dose. At $5x10^{14}$ cm^{-2}, there is only slight disorder to the lattice (as observed by channeling) but extensive damage (to both MgO and O sublattices) after the highest dose ($2x10^{16}$ cm^{-2}). However, even at the highest dose the MgO retains some crystalline order in the near-surface, i.e. it is not rendered amorphous by the implantation. Extracting the depth information from Fig. 6[17], gives the peak of the damage distribution at about 1000 Å below the surface but a measurable disorder to a depth of about 2500 Å. This is in agreement with ion implantation simulations using the code TRIM[18].

The channeling data are consistent with implantation damage previously observed in MgO[19,20], where point defect clusters, interstitial dislocation loops and polygonisation have been observed, but it is difficult to observe amorphous layers. Such defects can significantly effect both the mechanical behaviour of the near-surface layer (as indicated by improved hardness following implantation[21]) and the micromechanisms of crack nucleation. Disorder mostly leads to a compressive stress[19] in this surface layer, which is superimposed on thermal compressive stresses arising during the heating period of the thermal shock cycle.

A compressive plastic flow, taking place during heating in a layer highly saturated with ion beam induced dislocations and point defects, can activate a number of dislocation mechanisms contributing to microcrack nucleation. Multiple dislocation pile-ups along different crystallographic directions are likely to produce many submicroscopic cracks and voids[22]. During the heating stage the defects accumulate into appropriate crack nucleating sites. However, because of the compressive stresses acting during heating, the cracks are unlikely to grow and propagate. Nevertheless, they make fracture initiation and propagation easier during the cooling stage when tensile stresses appear. A high density of microcracks and voids is expected to reduce the fracture stress, while a high density of dislocations, point defects and microcracks suppresses plastic strain, thus making the relaxation of tensile stresses possible only by fracture. These factors should reduce the temperature threshold of cracking and facilitate multiple fragmentation as illustrated by the experimental results for

MgO crystals in Fig. 4. Thus, following ion implantation MgO monocrystals reduce their thermal shock resistance parameter. At the same time, as a consequence of a high crack density, their damage resistance parameter is increased[11-14].

The temperature threshold of cracking versus implantation dose in the range from $5x10^{14}$ cm^{-2} to 10^{17} cm^{-2} for glass samples is presented in Fig. 7. The characteristic feature of the dependence is that, at small doses, the ion implanted samples display higher thermal shock resistance than the unimplanted ones, whereas at doses higher than ~ 10^{16} cm^{-2} the situation is reversed. Such behaviour is obviously related to a competition between different processes associated with ion beam induced structure changes in glass. Indeed, glass can expand or contract under ion bombardment[23], depending on ion dose and the initial structure of the glass, leading to compressive or tensile stresses. In the case of implantation-induced contraction, the tensile stresses are formed in the near-surface layer. They should reduce overall compressive stresses during the heating stage, thus increasing the temperature threshold of fracture in glass. However, at large doses the structural damage is obviously a major factor which leads to the reduction of the thermal stress resistance parameter in glass. The behaviour we observe in glass may relate to such effects, but further experiments are needed to clarify this.

The significance of high crack density achieved by ion implantation lies in the possibility of improving the resistance to thermal shock damage in brittle materials. The degree of damage is commonly characterised by the depth of crack penetration following thermal shock. The latter quantity is highly dependent on crack density. High density crack systems tend to arrest fracture in a relatively thin surface layer, since their growth requires the absorption of a large amount of elastic energy, produced by tensile stresses during cooling[12,13]. In the case of small crack density, the elastic energy is commonly consumed by long cracks growing deep into the crystal interior. As analysed by Hasselman and Singh[13], a high density of microcracks can also favourably affect a number of mechanical and thermal properties of brittle ceramics.

4. CONCLUSION

This paper has shown that ion implantation has a significant affect on the behaviour of brittle materials under thermal shock generated by a plasma. Measurements of the gap between adjacent fragments have been used to estimate the surface temperature. Ion implantation is shown to modify the near-surface structure by introducing damage, which makes crack initiation easier under thermal stress in magnesia crystals. The fracture threshold and maximum crack density are shifted towards the lower temperature range. The thermal stress resistance parameter of glass samples is increased at relatively small doses and decreased at higher doses. The results suggest that crack density and the degree of damage in brittle ceramics operating under thermal shock conditions can be effectively controlled by ion implantation.

Acknowledgments.

Thanks are due to Mr. A. Orlov for his assistance with the experiments.

References.

1 Advances in Fracture Research, Proc. 7th Conf. on Fracture, Houston, TX, 1989, edited by K. Salama, K. Ravi-Chandar, D.M.R. Taplin and P. Rama Rao (Pergamon Press, Oxford, 1989).

2 C.C. Berndt, J. Mat. Sci. 24, 3511 (1989).

3 Y.R. Wang and T.W. Chou, J. Mat. Sci. 26, 2961 (1991).

4 P.D. Harmsworth and R. Stevens, J. Mat. Sci. 26, 3991 (1991).

5 I. Thompson and R.D. Rawlings, J. Mat. Sci., 26, 4534 (1991)

6 F. Osterstock, Mat. Sci.and Eng., A168, 41-44 (1993)

7 V. Finkel, V. Gurarie and N. Alushina, Doklady Academii Nauk SSSR, 7, No 3,1969.

8 F. Clarke, R. Sambell and J. Miles, Trans. of Brit. Ceram. Soc., 60, 299, 1961.

9 R. Dugdale, I. Maskrey and R. McVickers, Trans. of Brit. Ceram. Soc., 60, 427,1961.

10 G. D. Miles and F. J. P. Clarke, Phil. Mag.,6, 1449, 1961.

11 V. N. Gurarie and J. S. Williams, Journal of Materials Research, 5, No. 6, pp. 1257-1265, 1990.

12 D.P.H. Hasselman, Materials Science and Engineering, 71, pp. 251-264, 1985.

13 D.P.H. Hasselman and J.P. Singh, American Ceramic Society Bull., 58, No.9, pp. 856-860, 1979.

14 D. P.H. Hasselman, J. Am. Cer. Soc., 46, 11, 535-540, 1963.

15 V. Gurarie, Metals Forum. 7, 1, 12-21, 1984.

16 J.R. Hague, J.F. Lynch, A Rudnick, F.C. Holden, and W.H. Duckworth, In "Refractory Ceramics for Airspace", The American Ceramic Society, Inc. 1964.

17 W.K Chu, J.W. Mayer and M.A. Nicolet, "Rutherford Backscattering Spectrometry", Academic Press, N.Y., 1978.

18 J. F. Ziegler, J. P. Biersack and U. Littmark, in "The Stopping and Range of Ions in Matter", ed. J. F. Ziegler, Pergamon., New York, 1985.

19 C.W. White, C.J. McHargue, P.S. Sklad, L.A. Boatner and G.C. Farlow, Materials Science Reports, 4, 41, 1989.

20 Hj. Matzke and J.L. Whitton, Can. J. Phys., 44, 995 (1966)

21 P.J. Barnett and T.F. Page, J. Mater. Sci., 19, 3524, 1984.

22 V. Finkel, In "Fhysics of Fracture", Fizika Razrushenia, ed. Metallurgia, Moscow, 1970 (in Russian).

23 C.J. McHargue, in Ion Implantation 1988 ed. F.H. Wohlbrer (Trans. Tech. Publ. Aedernannsdorf, Switz.,1988), p. 359.

CAPTIONS FOR FIGURES.

Fig. 1 Fracture patterns of (a) MgO crystal and (b) glass sample at the border between the ion-implanted and unimplanted regions.

Fig. 2 Scanning electron micrographs showing adjacent fragments in (a) MgO and (b) glass samples.

Fig. 3 Fracture temperature versus distance r from the centre of the plasma affected area.

Fig. 4 Crack density in MgO as a function of peak surface temperature.

Fig. 5 Maximum fragment density as a function of implantation dose for ion-implanted and unimplanted MgO crystals.

Fig. 6 Rutherford backscattering and channeling spectra (using 2 MeV He^+) of implanted MgO monocrystals.

Fig. 7 The difference in thermal shock resistance parameter (TSRP) for ion implanted and unimplanted glass samples as a function of implantation dose. TSRP for unimplanted glass is ~120 ^{0}C.

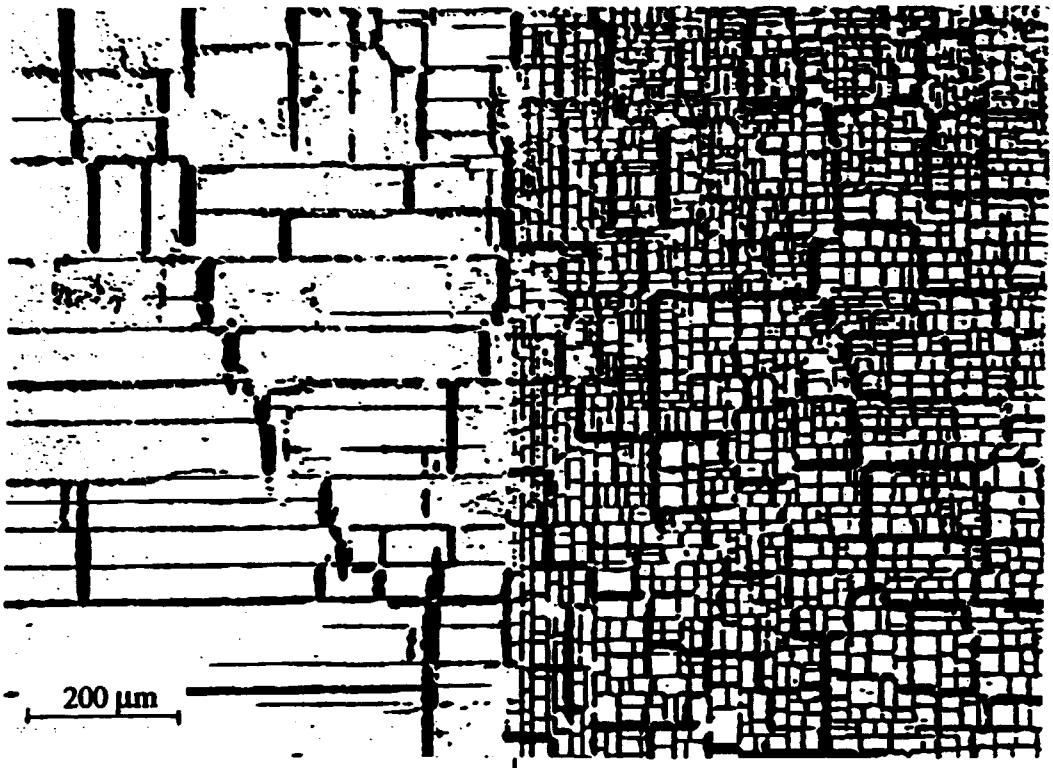

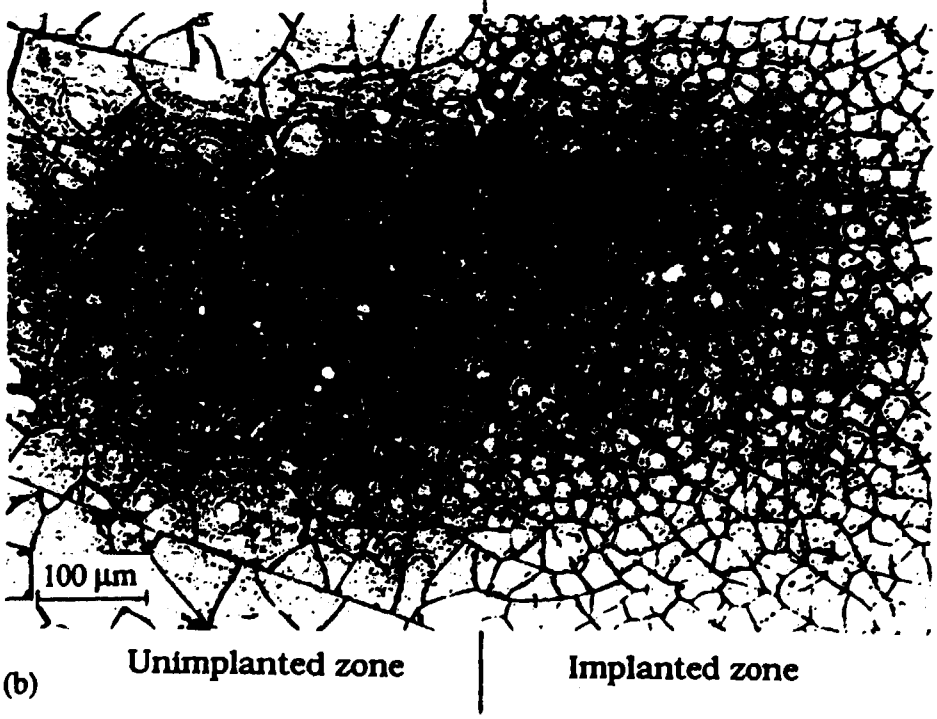

Fig. 1 Fracture patterns of (a) MgO crystal and (b) glass sample at the border between the ion-implanted and unimplanted regions.

2. a

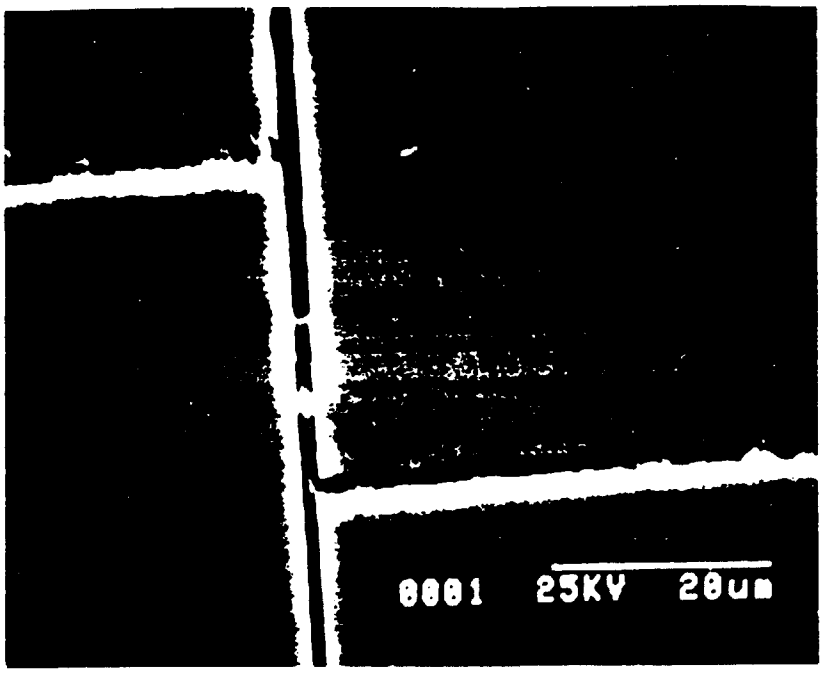

2, b

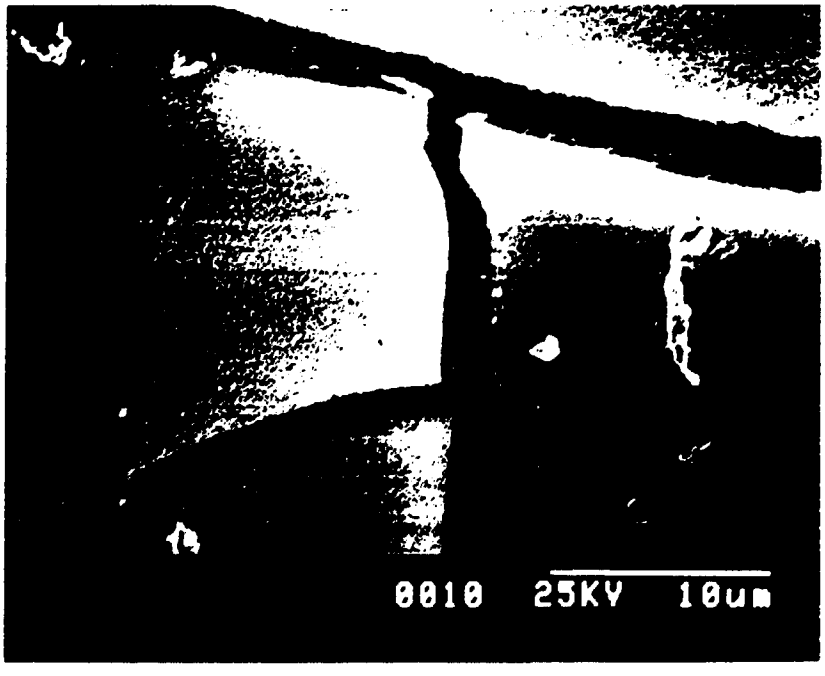

Fig. 2 Scanning electron micrographs showing adjacent fragments in (a) MgO and (b) glass samples.

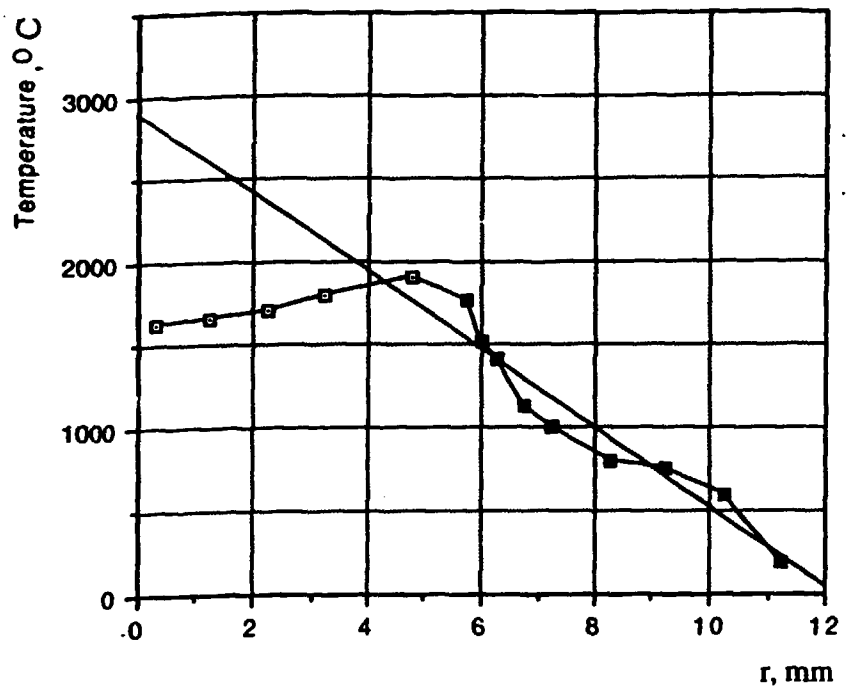

Fig. 3 Fracture temperature versus distance r from the centre of the plasma affected area.

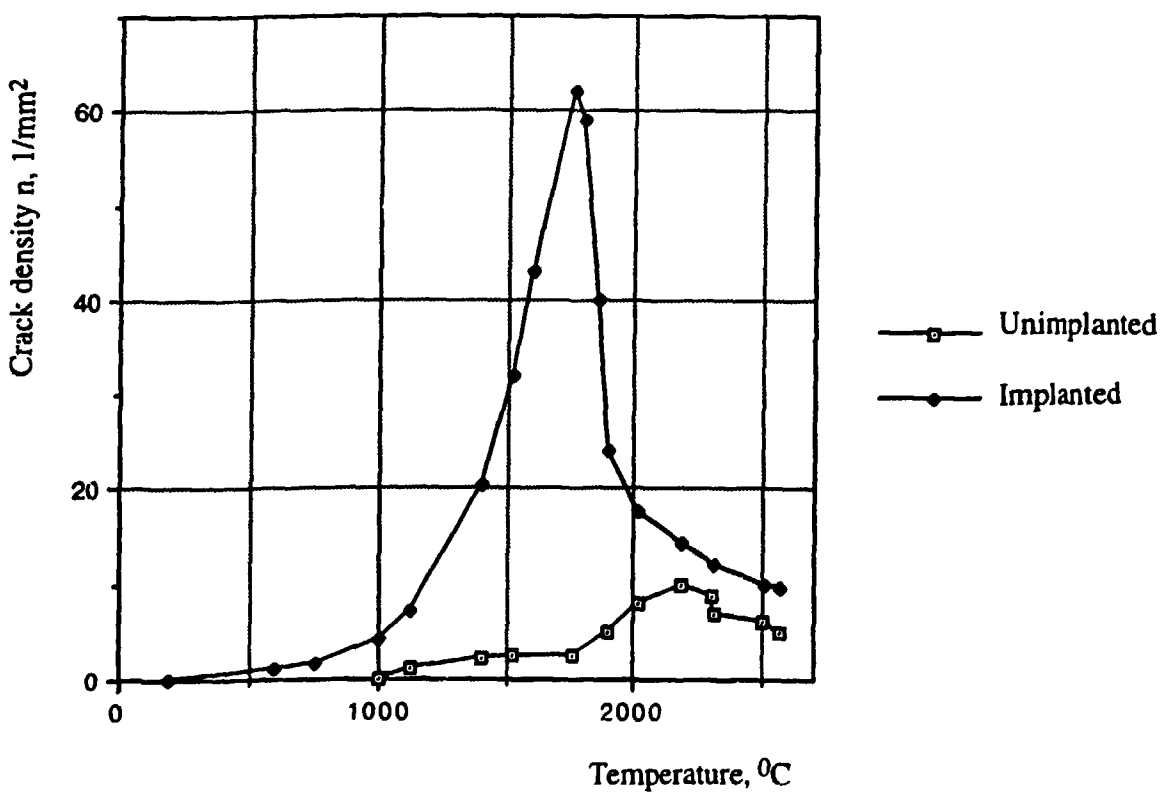

Fig. 4 Crack density in MgO as a function of peak surface temperature.

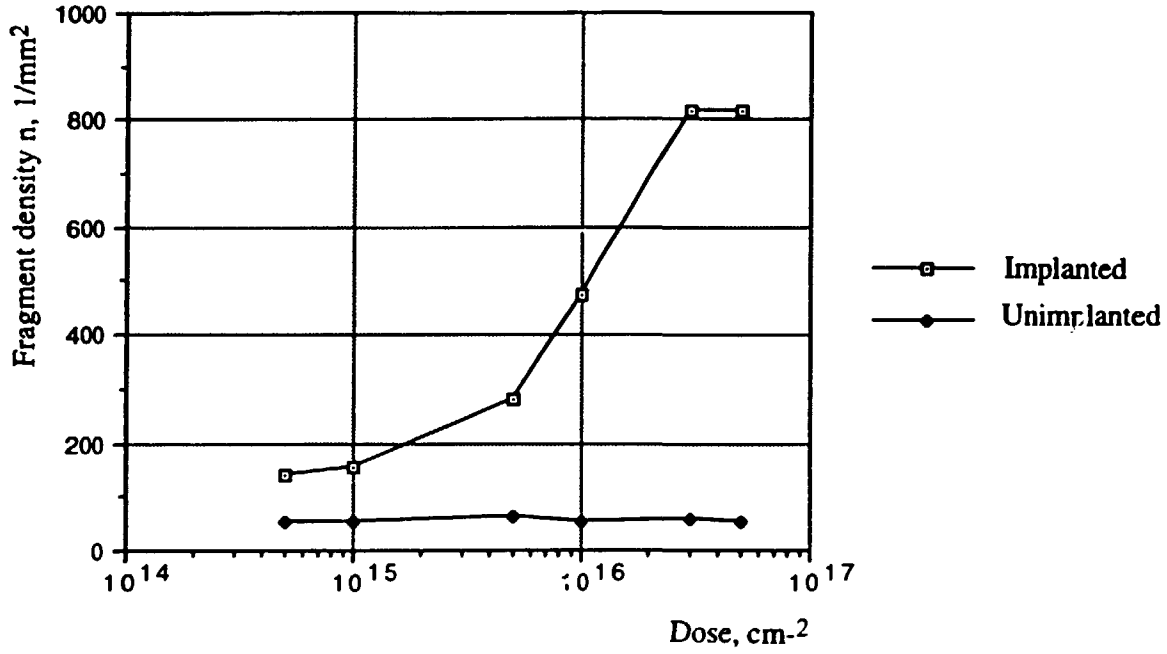

Fig. 5 Maximum fragment density as a function of implantation dose for ion-implanted and unimplanted MgO crystals.

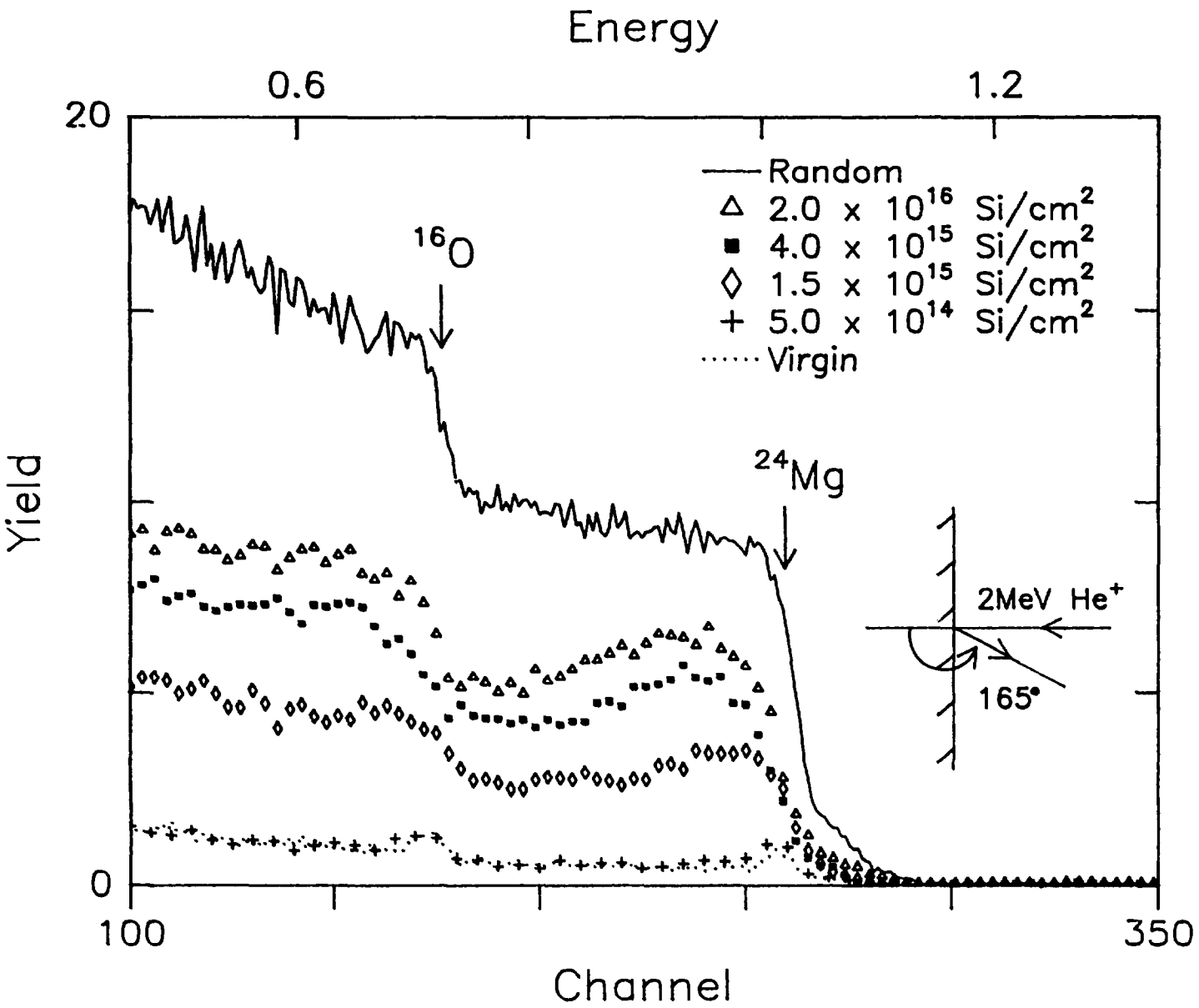

Fig. 6 Rutherford backscattering and channeling spectra (using 2 MeV He^+) of implanted MgO monocrystals.

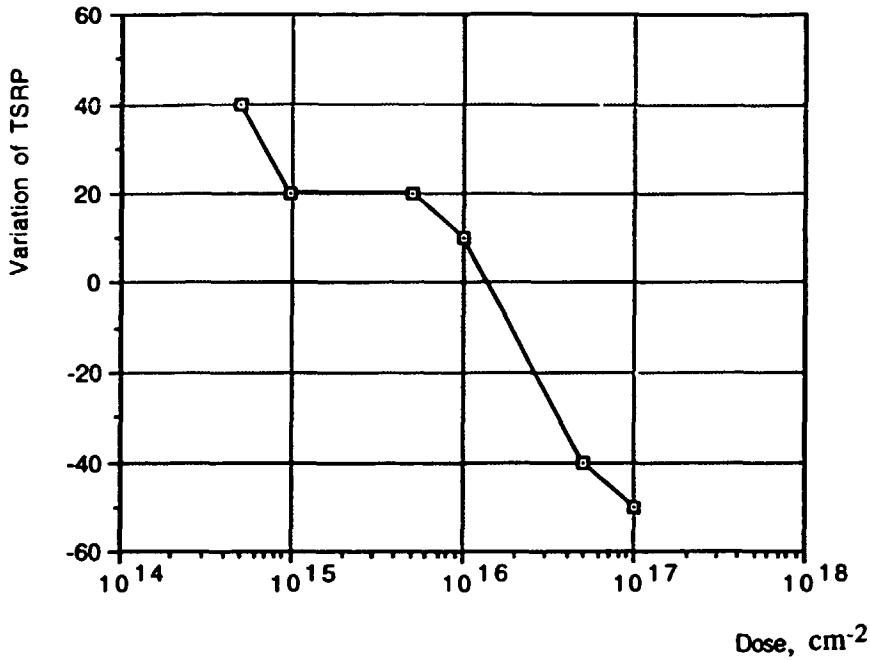

Fig. 7 The difference in thermal shock resistance parameter (TSRP) for ion implanted and unimplanted glass samples as a function of implantation dose. TSRP for unimplanted glass is ~120 ^{0}C.